

# Secure SWIPT Networks Based on a Non-linear Energy Harvesting Model

(Invited Paper)

Elena Boshkovska, Nikola Zlatanov, Linglong Dai, Derrick Wing Kwan Ng, and Robert Schober

**Abstract**—We optimize resource allocation to enable communication security in simultaneous wireless information and power transfer (SWIPT) for internet-of-things (IoT) networks. The resource allocation algorithm design is formulated as a non-convex optimization problem. We aim at maximizing the total harvested power at energy harvesting (EH) receivers via the joint optimization of transmit beamforming vectors and the covariance matrix of the artificial noise injected to facilitate secrecy provisioning. The proposed problem formulation takes into account the non-linearity of energy harvesting circuits and the quality of service requirements for secure communication. To obtain a globally optimal solution of the resource allocation problem, we first transform the resulting non-convex sum-of-ratios objective function into an equivalent objective function in parametric subtractive form, which facilitates the design of a novel iterative resource allocation algorithm. In each iteration, the semidefinite programming (SDP) relaxation approach is adopted to solve a rank-constrained optimization problem optimally. Numerical results reveal that the proposed algorithm can guarantee communication security and provide a significant performance gain in terms of the harvested energy compared to existing designs which are based on the traditional linear EH model.

## I. INTRODUCTION

In the era of the Internet of Things (IoT), it is expected that 50 billion wireless communication devices will be connected worldwide [1]. Smart physical objects equipped with sensors and wireless communication chips are able to collect and exchange information. These smart objects are wirelessly connected to computing systems to provide intelligent everyday services such as e-health, automated control, energy management (smart city and smart grid), logistics, security control, and safety management, etc. However, the limited energy storage capacity of battery-powered wireless communication devices severely limits the lifetime of wireless communication networks. Although battery replacement provides an intermediate solution to energy shortage, frequent replacement of batteries can be costly and cumbersome. This creates a serious performance bottleneck in providing stable communication services. On the other hand, a promising approach to extend the lifetime of wireless communication networks is to equip wireless communication devices with energy harvesting (EH) technology to scavenge energy from external sources. Solar, wind, tidal, biomass, and geothermal are the major renewable energy sources for generating electricity [2]. Yet, these conventional natural energy sources are usually climate and location

dependent which limits the mobility of the wireless devices. More importantly, the intermittent and uncontrollable nature of these natural energy sources is a major obstacle for providing stable wireless communications via traditional EH technologies.

Recently, wireless energy transfer (WET) has attracted significant attention from both academia and industry [3]–[11], as a key to unlock the potential of IoT. Generally speaking, the WET technology can be divided into three categories: magnetic resonant coupling, inductive coupling, and radio frequency (RF)-based WET. The first two technologies rely on near-field magnetic fields and do not support any mobility of EH devices, due to the short wireless charging distances and the required alignment of the magnetic field with the EH circuits. In contrast, RF-based WET technologies [3]–[11] utilize the far-field of electromagnetic (EM) waves which enables concurrent wireless charging and data communication in WET networks over long distances (e.g. hundreds of metres). Moreover, the broadcast nature of wireless channels facilitates one-to-many wireless charging which eliminates the need for power cords and manual recharging for IoT devices. As a result, simultaneous wireless information and power transfer (SWIPT) is expected to be a key enabler for sustainable IoT communication networks. Yet, the introduction of SWIPT to communication systems has led to a paradigm shift in both system architecture and resource allocation algorithm design. For instance, in SWIPT systems, one can increase the energy of the information carrying signal to increase the amount of RF energy harvested at the receivers. However, increasing the power of the information signals may also increase their susceptibility to eavesdropping, due to the higher potential for information leakage. As a result, both communication security concerns and the need for efficient WET naturally arise in systems providing SWIPT services.

Nowadays, various types of cryptographic encryption algorithms are employed at the application layer for guaranteeing wireless communication security. However, secure secret key management and distribution via an authenticated third party is typically required for these algorithms, which may not be realizable in future wireless IoT networks due to the expected massive numbers of devices. Therefore, a considerable amount of work has recently been devoted to information-theoretic physical (PHY) layer security as a complementary technology to the existing encryption algorithms [12]–[17]. It has been shown that in a wire-tap channel, if the source-destination channel enjoys better conditions compared to the source-eavesdropper channel [12], perfectly secure communication between a source and a destination is possible. Hence, multiple-antenna technology and advanced signal processing algorithms have been proposed to ensure secure communications. Specifically, by exploiting the extra degrees of freedom offered by multiple antennas, the information beams can be focused on the desired legitimate receivers to reduce the chance of information leakage. Besides, artificial noise can be injected into the communication channel deliberately to degrade the channel quality

E. Boshkovska and R. Schober are with Friedrich-Alexander-University Erlangen-Nürnberg (FAU), Germany. Linglong Dai is with Tsinghua University, Beijing, China. L. Dai is supported by the International Science & Technology Cooperation Program of China (Grant No. 2015DFG12760) and the National Natural Science Foundation of China (Grant No. 61571270). D. W. K. Ng is with The University of New South Wales, Australia. N. Zlatanov is with Monash University, Australia. R. Schober is supported by the AvH Professorship Program of the Alexander von Humboldt Foundation. D. W. K. Ng is supported under Australian Research Council's Scheme Discovery Early Career Researcher Award funding scheme (project number DE170100137).

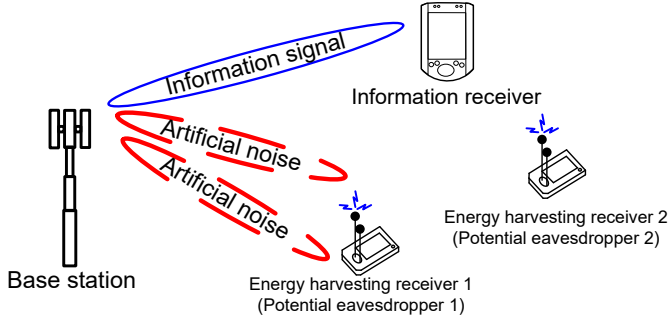


Fig. 1. A SWIPT model with an active IR and  $J = 2$  ERs. The ERs harvest wireless energy from the RF signal and are treated as potential eavesdroppers by the base station.

of eavesdroppers. These concepts have also been extended to SWIPT systems to provide secure communication. In [17], beamforming was studied to enhance security and power efficiency in SWIPT systems. The authors of [18] proposed a multi-objective optimization framework to investigate the non-trivial tradeoff between interference, total harvested power, and energy consumption in a secure cognitive radio SWIPT network. However, the resource allocation algorithms designed for secure SWIPT systems [17], [18] were based on a linear EH model which does not capture the highly non-linear characteristics of practical end-to-end WET [19]–[22]. In particular, existing resource allocation schemes designed for the linear EH model may lead to severe resource allocation mismatches resulting in performance degradation in WET and secure communications. These observations motivate us to study the design of efficient resource allocation algorithms for secure SWIPT systems taking into account a practical non-linear EH model.

## II. SYSTEM MODEL

In this section, we first introduce the notation adopted in this paper. Then, we present the downlink channel model for secure communication in SWIPT systems.

### A. Notation

We use boldface capital and lower case letters to denote matrices and vectors, respectively.  $\mathbf{A}^H$ ,  $\text{Tr}(\mathbf{A})$ ,  $\text{Rank}(\mathbf{A})$ , and  $\det(\mathbf{A})$  represent the Hermitian transpose, trace, rank, and determinant of matrix  $\mathbf{A}$ , respectively;  $\mathbf{A} \succ \mathbf{0}$  and  $\mathbf{A} \succeq \mathbf{0}$  indicate that  $\mathbf{A}$  is a positive definite and a positive semidefinite matrix, respectively;  $\mathbf{I}_N$  is the  $N \times N$  identity matrix;  $[\mathbf{q}]_{m:n}$  returns a vector with the  $m$ -th to the  $n$ -th elements of vector  $\mathbf{q}$ ;  $\mathbb{C}^{N \times M}$  denotes the set of all  $N \times M$  matrices with complex entries;  $\mathbb{H}^N$  denotes the set of all  $N \times N$  Hermitian matrices. The circularly symmetric complex Gaussian (CSCG) distribution is denoted by  $\mathcal{CN}(\mathbf{m}, \mathbf{\Sigma})$  with mean vector  $\mathbf{m}$  and covariance matrix  $\mathbf{\Sigma}$ ;  $\sim$  indicates “distributed as”;  $\mathcal{E}\{\cdot\}$  denotes statistical expectation;  $|\cdot|$  represents the absolute value of a complex scalar.  $[x]^+$  stands for  $\max\{0, x\}$  and  $[\cdot]^T$  represents the transpose operation.

### B. Channel Model

A frequency flat fading channel for downlink communication is considered. The SWIPT system comprises a base station (BS), an information receiver (IR), and  $J$  energy harvesting receivers (ER), as shown in Figure 1. The BS is equipped with  $N_T \geq 1$  antennas. The IR is a single-antenna device and each ER is equipped with  $N_R \geq 1$  receive antennas for EH. In the considered system, the signal intended for the IR is overheard by the ERs due to the broadcast nature of wireless channels.

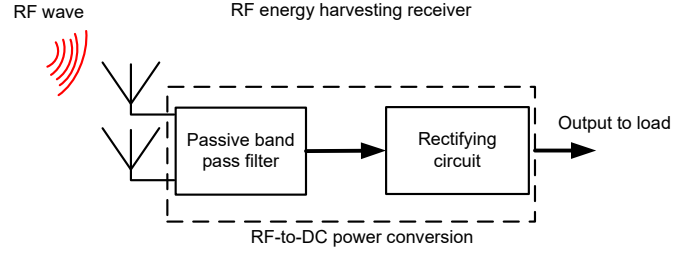


Fig. 2. Block diagram of an ER.

To guarantee communication security, the ERs are treated as potential eavesdroppers which has to be taken into account for resource allocation algorithm design. We assume that  $N_T > N_R$  for the following study. The signals received at the IR and ER  $j \in \{1, \dots, J\}$  are modelled as

$$y = \mathbf{h}^H(\mathbf{w}s + \mathbf{v}) + n, \quad (1)$$

$$y_{\text{ER}_j} = \mathbf{G}_j^H(\mathbf{w}s + \mathbf{v}) + \mathbf{n}_{\text{ER}_j}, \quad \forall j \in \{1, \dots, J\}, \quad (2)$$

respectively, where  $s \in \mathbb{C}$  and  $\mathbf{w} \in \mathbb{C}^{N_T \times 1}$  are the information symbol and the corresponding beamforming vector, respectively. Without loss of generality, we assume that  $\mathcal{E}\{|s|^2\} = 1$ .  $\mathbf{v} \in \mathbb{C}^{N_T \times 1}$  is an artificial noise vector generated by the BS to facilitate efficient WET and to guarantee communication security. In particular,  $\mathbf{v}$  is modeled as a random vector with circularly symmetric complex Gaussian distribution

$$\mathbf{v} \sim \mathcal{CN}(\mathbf{0}, \mathbf{V}), \quad (3)$$

where  $\mathbf{V} \in \mathbb{H}^{N_T}$ ,  $\mathbf{V} \succeq \mathbf{0}$ , denotes the covariance matrix of the artificial noise. The channel vector between the BS and the IR is denoted by  $\mathbf{h} \in \mathbb{C}^{N_T \times 1}$  and the channel matrix between the BS and ER  $j$  is denoted by  $\mathbf{G}_j \in \mathbb{C}^{N_T \times N_R}$ .  $n \sim \mathcal{CN}(0, \sigma_s^2)$  and  $\mathbf{n}_{\text{ER}_j} \sim \mathcal{CN}(\mathbf{0}, \sigma_s^2 \mathbf{I}_{N_R})$  are the additive white Gaussian noises (AWGN) at the IR and ER  $j$ , respectively, where  $\sigma_s^2$  denotes the noise power at each antenna of the receiver.

### C. Energy Harvesting Model

Figure 2 depicts the block diagram of the ER in SWIPT systems. In general, a bandpass filter and a rectifying circuit are adopted in an RF-ER to convert the received RF power to direct current (DC) power. The total received RF power at ER  $j$  is given by

$$P_{\text{ER}_j} = \text{Tr} \left( (\mathbf{w}\mathbf{w}^H + \mathbf{V}) \mathbf{G}_j \mathbf{G}_j^H \right). \quad (4)$$

In the SWIPT literature, for simplicity, the total harvested power at ER  $j$  is typically modelled as follows:

$$\Phi_{\text{ER}_j}^{\text{Linear}} = \eta_j P_{\text{ER}_j}, \quad (5)$$

where  $0 \leq \eta_j \leq 1$  denotes the energy conversion efficiency of ER  $j$ . From (5), it can be seen that with existing models, the total harvested power at the ER is linearly and directly proportional to the received RF power. However, practical RF-based EH circuits consist of resistors, capacitors, and diodes. Experimental results have shown that these circuits [19]–[21] introduce various non-linearities into the end-to-end WET. In order to design a resource allocation algorithm for practical secure SWIPT systems, we adopt the non-linear parametric EH model from [22], [23]. Consequently, the total harvested power

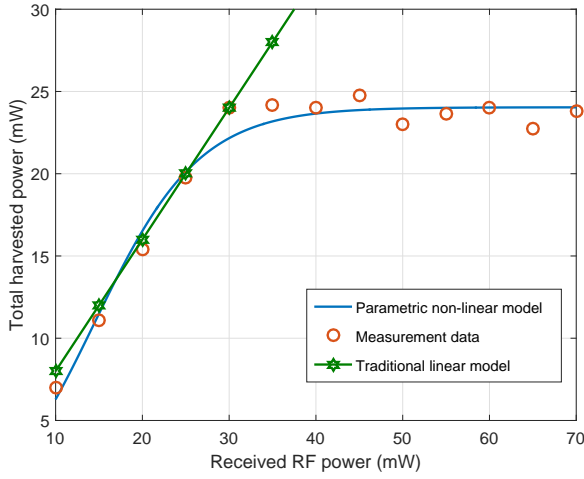


Fig. 3. A comparison between experimental data from [19], the harvested power for the non-linear model in (6), and the linear EH model with  $\eta_j = 0.8$  in (5).

at ER  $j$ ,  $\Phi_{ER_j}$ , is modelled as:

$$\Phi_{ER_j} = \frac{[\Psi_{ER_j} - M_j \Omega_j]}{1 - \Omega_j}, \quad \Omega_j = \frac{1}{1 + \exp(a_j b_j)}, \quad (6)$$

$$\text{where } \Psi_{ER_j} = \frac{M_j}{1 + \exp(-a_j(P_{ER_j} - b_j))} \quad (7)$$

is a sigmoid function which takes the received RF power,  $P_{ER_j}$ , as the input. Constant  $M_j$  denotes the maximal harvested power at ER  $j$  when the EH circuit is driven to saturation due to an exceedingly large input RF power. Constants  $a_j$  and  $b_j$  capture the joint effects of resistance, capacitance, and circuit sensitivity. In particular,  $a_j$  reflects the non-linear charging rate (e.g. steepness of the curve) with respect to the input power and  $b_j$  determines to the minimum turn-on voltage of the EH circuit. In practice, parameters  $a_j$ ,  $b_j$ , and  $M_j$  of the proposed model in (6) can be obtained using a standard curve fitting algorithm for measurement results of a given EH hardware circuit. In Figure 3, we show an example for the curve fitting for the non-linear EH model in (6) with parameters  $M = 0.024$ ,  $b = 0.014$ , and  $a = 150$ . It can be observed that the parametric non-linear model closely matches experimental results provided in [19] for the wireless power harvested by a practical EH circuit. Figure 3 also illustrates the inability of the linear model in (5) to capture the non-linear characteristics of practical EH circuits, especially in the high received RF power regime.

#### D. Secrecy Rate

Assuming perfect channel state information (CSI) is available at the receiver for coherent detection, the achievable rate (bit/s/Hz) between the BS and the IR is given by

$$R = \log_2 \left( 1 + \frac{\mathbf{w}^H \mathbf{H} \mathbf{w}}{\text{Tr}(\mathbf{H} \mathbf{V}) + \sigma_s^2} \right), \quad (8)$$

where  $\mathbf{H} = \mathbf{h} \mathbf{h}^H$ .

On the other hand, the capacity between the BS and ER  $j$  for decoding the signal of the IR can be expressed as

$$\begin{aligned} R_{ER_j} &= \log_2 \det(\mathbf{I}_{N_R} + \mathbf{Q}_j^{-1} \mathbf{G}_j^H \mathbf{w} \mathbf{w}^H \mathbf{G}_j), \quad (9) \\ \mathbf{Q}_j &= \mathbf{G}_j^H \mathbf{V} \mathbf{G}_j + \sigma_s^2 \mathbf{I}_{N_R} \succ \mathbf{0}, \end{aligned}$$

where  $\mathbf{Q}_j$  denotes the interference-plus-noise covariance matrix for ER  $j$ . Hence, the achievable secrecy rate of the IR is given by [14]

$$R_{\text{sec}} = \left[ R - \max_{\forall j} \{R_{ER_j}\} \right]^+. \quad (10)$$

### III. OPTIMIZATION PROBLEM AND SOLUTION

In the considered SWIPT system, we aim to maximize the total harvested power in the system while providing secure communication to the IR. To this end, we formulate the resource allocation algorithm design as the following non-convex optimization problem assuming that perfect channel state information is available<sup>1</sup>:

**Problem 1.** Resource Allocation for Secure SWIPT:

$$\begin{aligned} & \underset{\mathbf{V} \in \mathbb{H}^{N_T}, \mathbf{w}}{\text{maximize}} && \sum_{j=1}^J \Psi_{ER_j} \quad (11) \\ & \text{subject to} && \text{C1: } \|\mathbf{w}\|_2^2 + \text{Tr}(\mathbf{V}) \leq P_{\text{max}}, \\ & && \text{C2: } \frac{\mathbf{w}^H \mathbf{H} \mathbf{w}}{\text{Tr}(\mathbf{V} \mathbf{H}) + \sigma_s^2} \geq \Gamma_{\text{req}}, \\ & && \text{C3: } R_{ER_j} \leq R_{ER}^{\text{Tot}}, \forall j, \\ & && \text{C4: } \mathbf{V} \succeq \mathbf{0}. \end{aligned}$$

Constants  $P_{\text{max}}$  and  $\Gamma_{\text{req}}$  in constraints C1 and C2 denote the maximum transmit power budget and the minimum required signal-to-interference-plus-noise ratio (SINR) at the IR, respectively. Constant  $R_{ER}^{\text{Tot}} > 0$  in C3 is the maximum tolerable data rate which restricts the capacity of ER  $j$  if it attempts to decode the signal intended for the IR. In practice, the BS sets  $\log_2(1 + \Gamma_{\text{req}}) > R_{ER}^{\text{Tot}} > 0$ , to ensure secure communication<sup>2</sup>. Constraint C4 and  $\mathbf{V} \in \mathbb{H}^{N_T}$  constrain matrix  $\mathbf{V}$  to be a positive semidefinite Hermitian matrix. It can be observed that the objective function in (11) is a non-convex function due to its sum-of-ratios form. Besides, the log-det function in C3 is non-convex. Now, we first transform the non-convex objective function into an equivalent objective function in subtractive form via the following theorem.

**Theorem 1.** Suppose  $\{\mathbf{w}^*, \mathbf{V}^*\}$  is the optimal solution to (11), then there exist two column vectors  $\boldsymbol{\mu}^* = [\mu_1^*, \dots, \mu_J^*]^T$  and  $\boldsymbol{\beta}^* = [\beta_1^*, \dots, \beta_J^*]^T$  such that  $\{\mathbf{w}^*, \mathbf{V}^*\}$  is an optimal solution to the following optimization problem

$$\underset{\mathbf{V}^* \in \mathbb{H}^{N_T}, \mathbf{w}^* \in \mathcal{F}}{\text{maximize}} \sum_{j=1}^J \mu_j^* \left[ M_j - \beta_j^* \left( 1 + \exp(-a_j(P_{ER_j} - b_j)) \right) \right], \quad (12)$$

where  $\mathcal{F}$  is the feasible solution set of (11). Besides,  $\{\mathbf{w}^*, \mathbf{V}^*\}$  also satisfies the following system of equations:

$$\beta_j^* \left( 1 + \exp(-a_j(P_{ER_j}^* - b_j)) \right) - M_j = 0, \quad (13)$$

$$\mu_j^* \left( 1 + \exp(-a_j(P_{ER_j}^* - b_j)) \right) - 1 = 0, \quad (14)$$

and  $P_{ER_j}^* = \text{Tr} \left( (\mathbf{w}^* (\mathbf{w}^*)^H + \mathbf{V}^*) \mathbf{G}_j \mathbf{G}_j^H \right)$ .

*Proof:* Please refer to [24] for a proof of Theorem 1.  $\blacksquare$

<sup>1</sup>In the sequel, since  $\Omega_j$  does not affect the design of the optimal resource allocation policy, with a slight abuse of notation, we will directly use  $\Psi_{ER_j}$  to represent the harvested power at ER  $j$  for simplicity of presentation.

<sup>2</sup>In the considered problem formulation, we can guarantee that the achievable secrecy rate is bounded below by  $R_{\text{sec}} \geq \log_2(1 + \Gamma_{\text{req}}) - R_{ER}^{\text{Tot}} > 0$  if the problem is feasible.

TABLE I  
ITERATIVE RESOURCE ALLOCATION ALGORITHM.

### Algorithm

---

```

1: Initialize the maximum number of iterations  $L_{\max}$ , iteration index  $n = 0$ ,
 $\mu$ , and  $\beta$ 
2: repeat {Outer Loop}
3:   Solve the inner loop problem in (18) via semidefinite program relaxation
   for given  $(\mu^n, \beta^n)$  and obtain the intermediate beamformer  $\mathbf{w}'$  and
   artificial noise covariance matrix  $\mathbf{V}'$ 
4:   if (20) is satisfied then
5:     return Optimal beamformer  $\mathbf{w}^* = \mathbf{w}'$  and artificial noise covari-
     ance matrix  $\mathbf{V}^* = \mathbf{V}'$ 
6:   else
7:     Update  $\mu$  and  $\beta$  according to (19) and  $n = n + 1$ 
8:   end if
9: until (13) and (14) are satisfied or  $n = L_{\max}$ 

```

---

Therefore, for (11), we have an equivalent optimization problem in (12) with an objective function in subtractive form with extra parameters  $(\mu^*, \beta^*)$ . More importantly, the two problems have the same optimal solution  $\{\mathbf{w}^*, \mathbf{V}^*\}$ . Besides, the optimization problem in (12) can be solved by an iterative algorithm consisting of two nested loops [24]. In the inner loop, the optimization problem in (12) for given  $(\mu, \beta)$ ,  $\mu = [\mu_1, \dots, \mu_J]^T$  and  $\beta = [\beta_1, \dots, \beta_J]^T$ , is solved. Then, in the outer loop, we find the optimal  $(\mu^*, \beta^*)$  satisfying the system of equations in (13) and (14), cf. Algorithm 1 in Table I.

#### A. Solution of the Inner Loop Problem

In each iteration, in line 3 of Algorithm 1, we solve an inner loop optimization problem in its hypograph form:

#### Problem 2. Inner Loop Problem

$$\begin{aligned}
& \underset{\mathbf{W}, \mathbf{V} \in \mathbb{H}^{N_T}, \tau}{\text{maximize}} && \sum_{j=1}^J \mu_j^* \left[ M_j - \beta_j^* \left( 1 + \exp(-a_j(\tau_j - b_j)) \right) \right] \\
& \text{subject to} && \text{C1: } \text{Tr}(\mathbf{W} + \mathbf{V}) \leq P_{\max}, \\
& && \text{C2: } \frac{\text{Tr}(\mathbf{W}\mathbf{H})}{\Gamma_{\text{req}}} \geq \text{Tr}(\mathbf{V}\mathbf{H}) + \sigma_s^2, \\
& && \text{C3, C4,} \\
& && \text{C5: } \text{Tr} \left( (\mathbf{W} + \mathbf{V}) \mathbf{G}_j \mathbf{G}_j^H \right) \geq \tau_j, \forall j, \\
& && \text{C6: } \text{Rank}(\mathbf{W}) = 1, \text{ C7: } \mathbf{W} \succeq \mathbf{0}, \quad (15)
\end{aligned}$$

where  $\mathbf{W} = \mathbf{w}\mathbf{w}^H$  is a new optimization variable matrix and  $\tau = [\tau_1, \tau_2, \dots, \tau_J]$  is a vector of auxiliary optimization variables. The extra constraint C5 represents the hypograph of the inner loop optimization problem.

We note that the inner loop problem in (15) is still a non-convex optimization problem. In particular, the non-convexity arises from the log-det function in C3 and the combinatorial rank constraint C6. To circumvent the non-convexity, we first introduce the following proposition to handle constraint C3.

**Proposition 1.** For  $R_{\text{ER}}^{\text{Tot}} > 0, \forall j$ , and  $\text{Rank}(\mathbf{W}) \leq 1$ , constraint C3 is equivalent to constraint  $\overline{\text{C3}}$ , i.e.,

$$\text{C3} \Leftrightarrow \overline{\text{C3}}: \mathbf{G}_j^H \mathbf{W} \mathbf{G}_j \preceq \alpha_{\text{ER}} \mathbf{Q}_j, \forall j, \quad (16)$$

where  $\alpha_{\text{ER}} = 2^{R_{\text{ER}}^{\text{Tot}}} - 1$  is an auxiliary constant and  $\overline{\text{C3}}$  is a linear matrix inequality (LMI) constraint.

*Proof:* Please refer to Appendix A in [25] for the proof. ■

Now, we apply Proposition 1 to Problem (15) by replacing constraint C3 with constraint  $\overline{\text{C3}}$  which yields:

#### Problem 3. Equivalent Formulation of Problem (15)

$$\begin{aligned}
& \underset{\mathbf{W}, \mathbf{V} \in \mathbb{H}^{N_T}, \tau}{\text{maximize}} && \sum_{j=1}^J \mu_j^* \left[ M_j - \beta_j^* \left( 1 + \exp(-a_j(\tau_j - b_j)) \right) \right] \\
& \text{subject to} && \text{C1, C2, C4, C5, C7,} \\
& && \overline{\text{C3}}: \mathbf{G}_j^H \mathbf{W} \mathbf{G}_j \preceq \alpha_{\text{ER}} \mathbf{Q}_j, \forall j, \\
& && \text{C6: } \text{Rank}(\mathbf{W}) = 1. \quad (17)
\end{aligned}$$

The non-convexity of (17) is now only due to the rank constraint in C6. We adopt semidefinite programming (SDP) relaxation to obtain a tractable solution. Specifically, we remove the non-convex constraint C6 from (17) which yields:

#### Problem 4. SDP Relaxation of Problem (17)

$$\begin{aligned}
& \underset{\mathbf{W}, \mathbf{V} \in \mathbb{H}^{N_T}, \tau}{\text{maximize}} && \sum_{j=1}^J \mu_j^* \left[ M_j - \beta_j^* \left( 1 + \exp(-a_j(\tau_j - b_j)) \right) \right] \\
& \text{subject to} && \text{C1, C2, C4, C5, C7,} \\
& && \overline{\text{C3}}: \mathbf{G}_j^H \mathbf{W} \mathbf{G}_j \preceq \alpha_{\text{ER}} \mathbf{Q}_j, \forall j, \\
& && \text{C6: } \text{Rank}(\mathbf{W}) = 1. \quad (18)
\end{aligned}$$

In fact, (18) is a standard convex optimization problem which can be solved by numerical convex program solvers such as Sedumi or SDPT3 [26]. Now, we study the tightness of the adopted SDP relaxation in (18).

**Theorem 2.** For  $\Gamma_{\text{req}} > 0$  and if the considered problem is feasible, we can construct a rank-one solution of (17) based on the solution of (18).

*Proof:* Please refer to the Appendix. ■

Therefore, the non-convex optimization problem in (15) can be solved optimally.

#### B. Solution of the Outer Loop Problem

In this section, an iterative algorithm based on the damped Newton method is adopted to update  $(\mu, \beta)$  for the outer loop problem. For notational simplicity, we define functions  $\varphi_j(\beta_j) = \beta_j \left( 1 + \exp(-a_j(P_{\text{ER}_j} - b_j)) \right) - M_j$  and  $\varphi_{J+i}(\mu_i) = \mu_i \left( 1 + \exp(-a_i(P_{\text{ER}_i} - b_i)) \right) - 1$ ,  $i \in \{1, \dots, J\}$ . It is shown in [24] that the unique optimal solution  $(\mu^*, \beta^*)$  is obtained if and only if  $\varphi(\mu, \beta) = [\varphi_1, \varphi_2, \dots, \varphi_{2J}]^T = \mathbf{0}$ . Therefore, in the  $n$ -th iteration of the iterative algorithm,  $\mu^{n+1}$  and  $\beta^{n+1}$  can be updated as, respectively,

$$\begin{aligned}
\mu^{n+1} &= \mu^n + \zeta^n \mathbf{q}_{J+1:2J}^n \quad \text{and} \quad \beta^{n+1} = \beta^n + \zeta^n \mathbf{q}_{1:J}^n, \\
\text{where } \mathbf{q}^n &= [\varphi'(\mu, \beta)]^{-1} \varphi(\mu, \beta) \quad (19)
\end{aligned}$$

and  $\varphi'(\mu, \beta)$  is the Jacobian matrix of  $\varphi(\mu, \beta)$ .  $\zeta^n$  is the largest  $\varepsilon^l$  satisfying

$$\begin{aligned}
& \|\varphi(\mu^n + \varepsilon^l \mathbf{q}_{J+1:2J}^n, \beta^n + \varepsilon^l \mathbf{q}_{1:J}^n)\| \\
& \leq (1 - \eta \varepsilon^l) \|\varphi(\mu, \beta)\|, \quad (20)
\end{aligned}$$

where  $l \in \{1, 2, \dots\}$ ,  $\varepsilon^l \in (0, 1)$ , and  $\eta \in (0, 1)$ . The damped Newton method converges to the unique solution  $(\mu^*, \beta^*)$  satisfying the system of equations (13) and (14), cf. [24].

TABLE II  
SIMULATION PARAMETERS

System bandwidth	200 kHz
Carrier center frequency	915 MHz
Transceiver antenna gain	10 dBi
Number of receive antennas $N_R$	2
Noise power $\sigma^2$	-95 dBm
Maximum transmit power $P_{\max}$	36 dBm
BS-to-ER fading distribution	Rician with Rician factor 3 dB

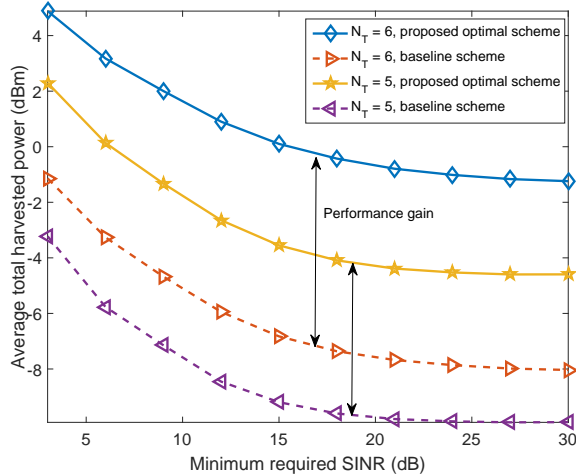


Fig. 4. Average total harvested power (dBm) versus the minimum required SINR (dB).

#### IV. RESULTS

In this section, simulation results are presented to illustrate the performance of the proposed resource allocation algorithm. We summarize the most important simulation parameters in Table II. In the simulation, the IR and the  $J = 10$  ERs are located at 50 meters and 10 meters from the BS, respectively. The maximum tolerable data rate at the potential eavesdropper is set to  $R_{\text{ER}}^{\text{Tot}} = 1$  bit/s/Hz. For the non-linear EH circuit, we set  $M_j = 20$  mW which corresponds to the maximum harvested power per ER. Besides, we adopt  $a_j = 6400$  and  $b_j = 0.003$ .

In Figure 4, we study the average total harvested power versus the minimum required receive SINR,  $\Gamma_{\text{req}}$ , at the IR for different numbers of transmit antennas and resource allocation schemes. As can be observed, the average total harvested power decreases with increasing  $\Gamma_{\text{req}}$ . Indeed, to satisfy a more stringent SINR requirement, the direction of information beam has to be steered towards the IR which yields a smaller amount of RF energy for EH at the ERs. On the other hand, a significant EH gain can be achieved by the proposed optimal scheme when the number of antennas equipped at the BS increases. In fact, additional transmit antennas equipped at the BS provide extra spatial degrees of freedom which facilitate a more flexible resource allocation. In particular, the BS can steer the direction of the artificial noise and the information signal towards the ERs accurately to improve the WET efficiency. For comparison, we also show the performance of a baseline scheme. For the baseline scheme, the resource allocation algorithm is designed based on an existing linear EH model, cf. (5). Specifically, we optimize  $\mathbf{w}, \mathbf{V}$  to maximize the total harvested power subject to the constraints in (11). Then, this baseline scheme is applied for resource allocation in the considered system with non-linear ERs. We observe from Figure 4 that a substantial performance gain is achieved by the proposed optimal resource allocation

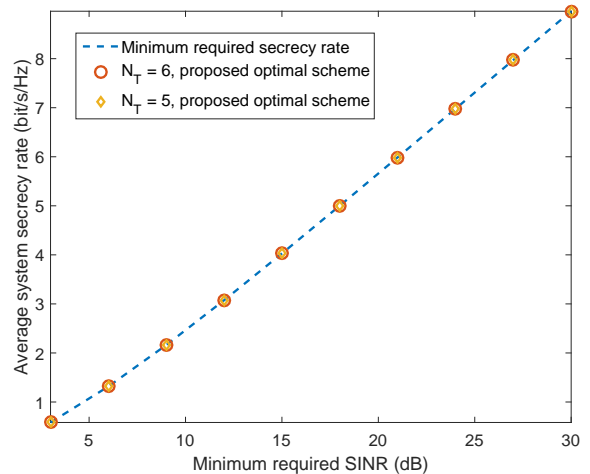


Fig. 5. Average system secrecy rate (bit/s/Hz) versus the minimum required SINR (dB).

algorithm compared to the baseline scheme. This is due to the fact that resource allocation mismatch occurs in the baseline scheme as it does not account for the non-linear nature of the EH circuits.

Figure 5 illustrates the average system secrecy rate versus the minimum required SINR  $\Gamma_{\text{req}}$  of the IR for different numbers of transmit antennas,  $N_T$ . The average system secrecy rate, i.e.,  $C_{\text{sec}}$ , increases with increasing  $\Gamma_{\text{req}}$ . This is because the maximum achievable rate of the ERs for decoding the IR signal is limited by the resource allocation to be less than  $R_{\text{ER}}^{\text{Tot}} = 1$  bit/s/Hz. Besides, although the minimum SINR requirement increases in Figure 5, the proposed optimal scheme is able to fulfill all QoS requirements due to the proposed optimization framework.

#### V. CONCLUSIONS

In this paper, a resource allocation algorithm enabling secure SWIPT in IoT communication networks was presented. The algorithm design based on a practical non-linear EH model was formulated as a non-convex optimization problem for the maximization of the total energy transferred to the ERs. We transformed the resulting non-convex optimization problem into two nested optimization problems which led to an efficient iterative approach for obtaining the globally optimal solution. Numerical results unveiled the potential performance gain in EH brought by the proposed optimization and its robustness against eavesdropping for IoT applications.

#### APPENDIX-PROOF OF THEOREM 2

To start with, we first define  $\tau^*$  as the optimal objective value of (18). When  $\text{Rank}(\mathbf{W}) > 1$  holds after solving (18), an optimal rank-one solution for (18) can be constructed as follows [27]. For a given  $\tau^*$ , we solve an auxiliary optimization problem:

$$\begin{aligned} & \underset{\mathbf{W}, \mathbf{V} \in \mathbb{H}^{N_T}}{\text{minimize}} && \text{Tr}(\mathbf{W}) && (21) \\ & \text{subject to} && C1, C2, \overline{C3}, C4, C5, C7. \end{aligned}$$

It can be observed that the optimal solution of (21) is also an optimal resource optimal resource allocation policy for (18) when  $\tau^*$  is fixed in (21). Therefore, in the remaining part of the proof, we show that solving (21) returns a rank-one

beamforming matrix  $\mathbf{W}$ . Therefore, we study the Lagrangian of problem (21) which is given by:

$$\begin{aligned}
L &= \text{Tr}(\mathbf{W}) + \lambda(\text{Tr}(\mathbf{W} + \mathbf{V}) - P_{\max}) - \text{Tr}(\mathbf{W}\mathbf{R}) \\
&- \sum_{j=1}^J \rho_j \left( \tau_j^* - \text{Tr} \left( (\mathbf{W} + \mathbf{V}) \mathbf{G}_j \mathbf{G}_j^H \right) \right) - \text{Tr}(\mathbf{V}\mathbf{Z}) \\
&+ \sum_{j=1}^J \text{Tr}(\mathbf{D}_{C_{3j}} (\mathbf{G}_j^H \mathbf{W} \mathbf{G}_j - \alpha_{\text{ER}} \mathbf{Q}_j)) \\
&+ \alpha \left( \text{Tr}(\mathbf{V}\mathbf{H}) + \sigma_s^2 - \frac{\text{Tr}(\mathbf{W}\mathbf{H})}{\Gamma_{\text{req}}} \right) + \Delta, \quad (22)
\end{aligned}$$

where  $\lambda \geq 0$ ,  $\alpha \geq 0$ ,  $\mathbf{D}_{C_{3j}} \succeq \mathbf{0}, \forall j \in \{1, \dots, J\}$ ,  $\mathbf{Z} \succeq \mathbf{0}$ ,  $\rho_j \geq 0$ , and  $\mathbf{R} \succeq \mathbf{0}$  are the dual variables for constraints C1, C2, C3, C4, C5, and C7, respectively.  $\Delta$  is a collection of variables and constants that are not relevant to the proof.

Then, we exploit the following Karush-Kuhn-Tucker (KKT) conditions which are needed for the proof<sup>3</sup>:

$$\mathbf{R}^*, \mathbf{Z}^*, \mathbf{D}_{C_{3j}}^* \succeq \mathbf{0}, \quad \lambda^*, \alpha, \rho_j^* \geq 0, \quad (23)$$

$$\mathbf{R}^* \mathbf{W}^* = \mathbf{0}, \quad \mathbf{Z}^* \mathbf{V}^* = \mathbf{0}, \quad (24)$$

$$\begin{aligned}
\mathbf{R}^* &= (\lambda^* + 1) \mathbf{I}_{N_T} - \sum_{j=1}^J \rho_j \mathbf{G}_j \mathbf{G}_j^H + \sum_{j=1}^J \mathbf{G}_j \mathbf{D}_{C_{3j}}^* \mathbf{G}_j^H \\
&- \alpha^* \frac{\mathbf{H}}{\Gamma_{\text{req}}}, \quad (25)
\end{aligned}$$

$$\begin{aligned}
\mathbf{Z}^* &= \lambda^* \mathbf{I}_{N_T} - \sum_{j=1}^J \rho_j \mathbf{G}_j \mathbf{G}_j^H \\
&- \sum_{j=1}^J \alpha_{\text{ER}} \mathbf{G}_j \mathbf{D}_{C_{3j}}^* \mathbf{G}_j^H + \alpha^* \mathbf{H}. \quad (26)
\end{aligned}$$

Then, subtracting (26) from (25) yields

$$\begin{aligned}
\mathbf{R}^* &= \underbrace{\mathbf{I}_{N_T} + \mathbf{Z}^* + \sum_{j=1}^J (1 + \alpha_{\text{ER}}) \mathbf{G}_j \mathbf{D}_{C_{3j}}^* \mathbf{G}_j^H}_{\mathbf{A} \succ \mathbf{0}} \\
&- \alpha^* \mathbf{H} \left( 1 + \frac{1}{\Gamma_{\text{req}}} \right). \quad (27)
\end{aligned}$$

Besides, constraint C2 in (21) is satisfied with equality for the optimal solution and we have  $\alpha^* > 0$ . From (27), we have

$$\begin{aligned}
&\text{Rank}(\mathbf{R}^*) + \text{Rank}(\alpha^* \mathbf{H} (1 + 1/\Gamma_{\text{req}})) \\
&\geq \text{Rank}(\mathbf{R}^* + \alpha^* \mathbf{H} (1 + 1/\Gamma_{\text{req}})) \\
&= \text{Rank}(\mathbf{A}) = N_T \\
&\Rightarrow \text{Rank}(\mathbf{R}^*) \geq N_T - 1. \quad (28)
\end{aligned}$$

As a result,  $\text{Rank}(\mathbf{R}^*)$  is either  $N_T - 1$  or  $N_T$ . Furthermore, since  $\Gamma_{\text{req}} > 0$  in C2,  $\mathbf{W}^* \neq \mathbf{0}$  is necessary. Hence,  $\text{Rank}(\mathbf{R}^*) = N_T - 1$  and  $\text{Rank}(\mathbf{W}^*) = 1$  hold and the rank-one solution for (18) is constructed. ■

## REFERENCES

- [1] M. Zorzi, A. Gluhak, S. Lange, and A. Bassi, "From today's INTRANet of things to a Future INTERNet of Things: a Wireless- and Mobility-Related View," *IEEE Wireless Commun.*, vol. 17, pp. 44–51, 2010.
- [2] D. W. K. Ng, E. S. Lo, and R. Schober, "Energy-Efficient Resource Allocation in OFDMA Systems with Hybrid Energy Harvesting Base Station," *IEEE Trans. Wireless Commun.*, vol. 12, pp. 3412–3427, Jul. 2013.
- [3] P. Grover and A. Sahai, "Shannon Meets Tesla: Wireless Information and Power Transfer," in *Proc. IEEE Intern. Sympos. on Inf. Theory*, Jun. 2010, pp. 2363–2367.
- [4] I. Krikidis, S. Timotheou, S. Nikolaou, G. Zheng, D. W. K. Ng, and R. Schober, "Simultaneous Wireless Information and Power Transfer in Modern Communication Systems," *IEEE Commun. Mag.*, vol. 52, no. 11, pp. 104–110, Nov. 2014.
- [5] Z. Ding, C. Zhong, D. W. K. Ng, M. Peng, H. A. Suraweera, R. Schober, and H. V. Poor, "Application of Smart Antenna Technologies in Simultaneous Wireless Information and Power Transfer," *IEEE Commun. Mag.*, vol. 53, no. 4, pp. 86–93, Apr. 2015.
- [6] X. Chen, Z. Zhang, H.-H. Chen, and H. Zhang, "Enhancing Wireless Information and Power Transfer by Exploiting Multi-Antenna Techniques," *IEEE Commun. Mag.*, no. 4, pp. 133–141, Apr. 2015.
- [7] X. Chen, D. W. K. Ng, and H.-H. Chen, "Secrecy Wireless Information and Power Transfer: Challenges and Opportunities," *IEEE Commun. Mag.*, 2016.
- [8] Q. Wu, M. Tao, D. Ng, W. Chen, and R. Schober, "Energy-Efficient Resource Allocation for Wireless Powered Communication Networks," *IEEE Trans. Wireless Commun.*, vol. 15, pp. 2312–2327, Mar. 2016.
- [9] X. Chen, X. Wang, and X. Chen, "Energy-Efficient Optimization for Wireless Information and Power Transfer in Large-Scale MIMO Systems Employing Energy Beamforming," *IEEE Wireless Commun. Lett.*, vol. 2, pp. 1–4, Dec. 2013.
- [10] R. Zhang and C. K. Ho, "MIMO Broadcasting for Simultaneous Wireless Information and Power Transfer," *IEEE Trans. Wireless Commun.*, vol. 12, pp. 1989–2001, May 2013.
- [11] Q. Wu, W. Chen, and J. Li, "Wireless Powered Communications With Initial Energy: QoS Guaranteed Energy-Efficient Resource Allocation," *IEEE Wireless Commun. Lett.*, vol. 19, Dec. 2015.
- [12] A. D. Wyner, "The Wire-Tap Channel," Tech. Rep., Oct. 1975.
- [13] J. Zhu, R. Schober, and V. Bhargava, "Secure Transmission in Multicell Massive MIMO Systems," *IEEE Trans. Wireless Commun.*, vol. 13, pp. 4766–4781, Sep. 2014.
- [14] S. Goel and R. Negi, "Guaranteeing Secrecy using Artificial Noise," *IEEE Trans. Wireless Commun.*, vol. 7, pp. 2180–2189, Jun. 2008.
- [15] H. M. Wang, C. Wang, D. Ng, M. Lee, and J. Xiao, "Artificial Noise Assisted Secure Transmission for Distributed Antenna Systems," *IEEE Trans. Signal Process.*, vol. PP, no. 99, pp. 1–1, 2016.
- [16] J. Chen, X. Chen, W. H. Gerstacker, and D. W. K. Ng, "Resource Allocation for a Massive MIMO Relay Aided Secure Communication," *IEEE Trans. on Inf. Forensics and Security*, vol. 11, no. 8, pp. 1700–1711, Aug. 2016.
- [17] D. W. K. Ng, E. S. Lo, and R. Schober, "Robust Beamforming for Secure Communication in Systems with Wireless Information and Power Transfer," *IEEE Trans. Wireless Commun.*, vol. 13, pp. 4599–4615, Aug. 2014.
- [18] —, "Multiobjective Resource Allocation for Secure Communication in Cognitive Radio Networks With Wireless Information and Power Transfer," *IEEE Trans. Veh. Technol.*, vol. 65, no. 5, pp. 3166–3184, May 2016.
- [19] J. Guo and X. Zhu, "An Improved Analytical Model for RF-DC Conversion Efficiency in Microwave Rectifiers," in *IEEE MTT-S Int. Microw. Symp. Dig.*, Jun. 2012, pp. 1–3.
- [20] C. Valenta and G. Durgin, "Harvesting Wireless Power: Survey of Energy-Harvester Conversion Efficiency in Far-Field, Wireless Power Transfer Systems," *IEEE Microw. Mag.*, vol. 15, pp. 108–120, Jun. 2014.
- [21] T. Le, K. Mayaram, and T. Fiez, "Efficient Far-Field Radio Frequency Energy Harvesting for Passively Powered Sensor Networks," *IEEE J. Solid-State Circuits*, vol. 43, pp. 1287–1302, May 2008.
- [22] E. Boshkovska, D. Ng, N. Zlatanov, and R. Schober, "Practical Non-Linear Energy Harvesting Model and Resource Allocation for SWIPT Systems," *IEEE Commun. Lett.*, vol. 19, pp. 2082–2085, Dec. 2015.
- [23] E. Boshkovska, D. W. K. Ng, N. Zlatanov, A. Koelpin, and R. Schober, "Robust Resource Allocation for MIMO Wireless Powered Communication Networks Based on a Non-linear EH Model," 2016, submitted to TCOM. [Online]. Available: <http://arxiv.org/abs/1609.03836>
- [24] Y. Jong, "An Efficient Global Optimization Algorithm for Nonlinear Sum-of-Ratios Problem," May 2012. [Online]. Available: <http://www.optimization-online.org/DBFILE/2012/08/3586.pdf>
- [25] D. W. K. Ng, M. Shaqfeh, R. Schober, and H. Alnuweiri, "Robust Layered Transmission in Secure MISO Multiuser Unicast Cognitive Radio Systems," *IEEE Trans. Veh. Technol.*, vol. 65, no. 10, pp. 8267–8282, Oct. 2016.
- [26] M. Grant and S. Boyd, "CVX: Matlab Software for Disciplined Convex Programming, version 2.0 Beta," [Online] <https://cvxr.com/cvx>, Sep. 2013.
- [27] Y. Sun, D. W. K. Ng, J. Zhu, and R. Schober, "Multi-Objective Optimization for Robust Power Efficient and Secure Full-Duplex Wireless Communication Systems," *IEEE Trans. Wireless Commun.*, vol. 15, no. 8, pp. 5511–5526, Aug. 2016.

<sup>3</sup>In this proof, the optimal primal and dual variables of (21) are denoted by the corresponding variables with an asterisk superscript.